Effects of temperature and slope on the infiltration rate for landfill surface

Lohit Jain[1], Sumedha Chakma[2]

[1]*Department of Civil engineering, Indian Institute of Technology, Delhi, India;*

[2]*Department of Civil engineering, Indian Institute of Technology, Delhi, India*

Correspondence details:

Mr. Lohit Jain

House no. 194

Teacher Colony, Nimach (Postal code- 458441)

Madhya-Pradesh, India

Email id: ljbestnmh@gmail.com, cez148040@civil.iitd.ac.in

Effects of temperature and slope on the infiltration rate for landfill surface

In this study, the parameters of the Kostiakov, Horton, Modified-Kostiakov, SCS, Philip and Smith models were estimated based on the double-ring infiltrometer on two different slopes, 4^{o} and $23^{o,}$ in morning and afternoon sessions to assess their usefulness in characterising the infiltration process. Observations showed that the average increment in temperature by $9^{o}C$ increased the final and initial infiltration rates by 65% and 38%. Combined effects of 23^{o} slope and higher temperature increased the infiltrated volume 6.4 times. The comparative analysis showed Kostiakov as the most efficient model incorporating combined and individual effects of temperature and slope, among other models.

Keywords: Infiltration rate, temperature, landfill, double-ring infiltrometer, slope

Introduction

The rapid growth of industries and population has led to the net migration of people from villages and towns, including metropolitan cities resulting in a large amount of solid waste in metro cities[1]. The population in Delhi has increased from 13.9 million in 2001 to 16.8 million in 2011 and 30.3 million in 2020[2]. It has increased the solid waste generation from $1.05x10^{4}$ TPD (Tonnes per day) in 2016 to $1.11x10^{4}$ TPD in 2021[3,4]. Primarily, three landfill sites, Gazipur, Bhalswa and Okhla, were chosen for receiving solid waste over a total area of 60 hectares in Delhi[5]. The present study highlights the infiltration characteristics of the Okhla landfill, incorporating slope and temperature variations. Okhla landfill processes 1800 Tonnes per day (TPD) approximately, which is 51% of total solid waste generation (3600 TPD) in South Delhi in 2019-2020[6]. Dumping of solid waste is being managed so improperly that it has

created 40 meters of massive mountains against the permissible height of 20 meters with a spread of 46 acres area of solid waste[6].

The landfill is a heterogeneous system where infiltration is one of the prime causes of leachate generation[7]. The generated leachate significantly affects the hydraulic conductivity of the soil system, groundwater quality and nitrogen diminution[8]. It is established that field density, temperature variation, moisture content of top surface and type of wastes are the main factors that influence the process of infiltration and leachate generation[9,10].

Several experiments have been conducted to compare the suitability of the different models by comparing the model output and field observations[11,12]. In a field study, the dependency of the steady-state infiltration rate has shown weak correlations with textural variables and a strong correlation with the soil particles' structural arrangement[13]. In the last century, many physical, semi-empirical and empirical infiltration models have been developed[14]. The previous study reported that infiltration rates had been underestimated by the Philip model for the time longer than the experiment duration; however, steady-state infiltration rates predicted by the Horton model have been reported to be fairly accurate[15]. Model preciseness depends on soil characteristics, land use-landcover, temperature variation, slope and initial moisture content[16–19].

The effects of temperature variations and different surface inclinations were considered to be the governing factors for the infiltration experiments. Experimental data and theoretical studies have shown that temperature and slope of the surface significantly influence the hydrologic processes and infiltration mechanism, which have not been considered in classical infiltration models for any land use[20]. Infiltration is such a complex physical phenomenon that no single model has been found suitable for all the temperature ranges and slopes; hence it is hard to know the most appropriate model for a given condition[21].

Infiltration Models

Various Mathematical expressions have been proposed for describing the one-dimensional infiltration process. Some of the most common models were calibrated to investigate the effects of slope and temperature variation on the infiltration model parameters for the municipal solid waste landfill in Okhla (Table 1). The objective of this study was to inspect the individual and combined impact of diurnal temperature variation and slope on the infiltration process for municipal solid waste landfill and examine the variation in the parameters of six popular infiltration models for focused factors (slope and temperature). The study also includes the comparative analysis of classical infiltration models' outcomes to evaluate their suitability for the given slope and temperature variation conditions.

Materials and methods

Study area: Delhi is the capital of India, covering a 1483 KM^2 area. In the last 14 years, the highest annual rainfall has been recorded as 1530 mm in 2013, and yearly minimum rainfall was observed as 560 mm in 2012 with an average rainfall of 880 mm[22]. Delhi has a sub-tropical climate, where summers are very hot with temperatures attained till 45^oC and winters are very cold with temperatures falling to 2^oC. The annual average difference in maximum and minimum diurnal temperature in Delhi has been observed approximately 11^oC[23].

The present study and experiments were conducted at a non-engineered municipal solid waste landfill located at Okhla in Delhi, as shown in Figure 1(a), using double-ring infiltrometer, as shown in Figure 1(b). Okhla landfill site was commissioned in 1994 and owned by South Delhi Municipal Corporation for dumping solid waste. The dumped municipal waste was covered by a 45 cm to 60 cm thick soil layer to obstruct its direct exposure to the atmosphere[24].

Field Experiment

The ring infiltrometer is the most common instrument for measuring cumulative infiltration on

the field[25]. Three sets of Ring-infiltrometer experiments were performed on Okhla landfill during April - May 2016 on a plain surface (4^o) and slope (23^o) in afternoon and morning sessions for 3.5 to 4 hours to incorporate the diurnal temperature variation effect on the infiltration mechanism. The procedure of double-ring infiltrometer experiments was followed from the American Society for Testing and Materials (ASTM) manual[26]. The prime advantage of ring-infiltrometers is the feasibility of field experiments without conserving and collecting the samples from the site at an economical cost and lesser water consumption than rainfall simulators[27]. Dimensions for outer infiltrometer ring diameter, inner ring diameter and height of the rings (45x30x30 cm) were used for the field experiments in the following four conditions (a) Plain surface in the morning session (4^o slope, 26 ^{o}C-32 ^{o}C) (b) Plain surface in afternoon surface (4^o, 36^oC-42^oC) (c) Inclined surface in the morning session (23^o slope, 30^oC -35^oC) and (d) Inclined surface in the afternoon (23^o slope, 38^oC-42^oC). Experiments were performed in all mentioned conditions to observe the effect of temperature (condition b), slope (condition c) and combined effect (condition d) as compared to Condition 'a'. The temperature was measured near the surface by calibrated digital temperature meter (Model no. PW18183, HTC-1) for each infiltration observation. The ring was installed approximate 5 cm depth into the upper layer of soil by hammering the tray laid over the ring for the uniform impact. Observations were taken at the variable interval duration from 30 seconds to 1800 second based on the constant infiltration rate attained for each interval. Water was replenished with minimum turbulence after the water level falls about 4 to 5 cm in the ring. In a double ring experiment, the water level was kept the same in both rings during the experiment for the effective vertical infiltration. The experiment was carried out until a constant infiltration rate was obtained in 30 minutes interval observations. Table 2 presents the initial infiltration rate (f_o in cm/min), final infiltration rate (f_c in cm/min), slope and temperature (^{o}C) ranges during experiments in Okhla landfill.

The waste samples were collected from 20 cm depth near the experiment location, as

Shukla (2003) suggested[28]. Double-ring infiltrometer was hammered up to 5 cm in the ground to minimise soil disturbance[29]. The Soil matrix of 0 cm-20 cm depth plays a significant role in the orientation of the infiltration process. Experimental observations were analysed using soil characteristics from the top 20 cm soil; therefore, sampling from the variable depth was not chosen. Three sets of the particle size distribution, initial moisture content, specific gravity, liquid limit, plastic limit, falling head permeability, and standard proctor experiments in the laboratory and the core-cutter test in the field were performed to investigate the physical and hydraulic characteristics of the soil. The samples were carried from field to labs and stored in air-tight bags to preserve the moisture content. Soil particle distribution was investigated by sieve analysis (coarse particles) and hydrometer (fine particles). Total 3.3% weight of soil sample was lost during the experiments. Average soil characteristics were measured experimentally and shown in Table 3.

For the Okhla landfill, the variations of different types of densities, porosity and the void ratio were evaluated and presented in Figure 2 and Figure 3.

Performance assessment

Nash-Sutcliffe efficiency (NSE), Coefficient of determination (R^2), Percent bias (PBIAS) and Root Mean Square Error-observations standard deviation ratio (RSR) were selected for the model assessment and experimental comparison in the infiltration process for different scenarios[30].

If x-series and y-series represent the observed infiltration values and the simulated values, respectively and $\bar{x}$ is the mean values for the same series, NSE can be evaluated using Eq. (1),

$$NSE = 1 - \left[\frac{\sum_{i=1}^{n}(x-y)^2}{\sum_{i=1}^{n}(x-\overline{x})^2}\right] \quad (1)$$

142 R^2 explains the percentage of the variation in simulated infiltration rate and infiltrated
143 amount concerning observed results in terms of the degree of collinearity (Eq. 2)[31].

144 $$R^2 = \left[\frac{\sum_{i=1}^{n}(x-\overline{x})(y-\overline{y})}{\sum_{i=1}^{n}(x-\overline{x})^2 \sum_{i=1}^{n}(y-\overline{y})^2}\right]^2 \quad (2)$$

145 PBIAS was computed using Eq. 3, which measures the difference between the model
146 infiltration rate and corresponding experimental values[31].

147 $$PBIAS = \frac{\sum_{i=1}^{n}(x-\overline{y})100}{\sum_{i=1}^{n}(x)} \quad (3)$$

148 RSR was calculated using Eq. 4, which contains the advantages of error index statistics
149 and incorporates a normalising factor, so the resulting statistics and reported values can apply
150 to different output responses[31].

151 $$RSR = \left[\frac{\sum_{i=1}^{n}(x-y)^2}{\sum_{i=1}^{n}(x-\overline{x})^2}\right] \quad (4)$$

152 **Results**

153 Observed experimental data sets from each scenario for the duration of 3 to 4 hours were used
154 to generate and analyse the infiltration rate curves. Results of observed infiltration rates in
155 different scenarios are summarised in Figure 4. The initial infiltration rate did not show any
156 noticeable change from 26ºC-32ºC (morning session) to 36ºC-42ºC (afternoon session);
157 however, the final infiltration rate showed proportionality with mentioned temperature ranges
158 on the plain surface yet did not present any significant correlation. On the other hand, as the
159 slope increased from plain surface to 23º inclination, the initial-final infiltration rates were
160 increased approximately twice under ponded conditions, as mentioned in Table 2, which is
161 equivalent to the final infiltration rates ratio of 1.9 for the diurnal temperature variation from
162 14.9ºC to 31.5ºC [32]. Similar results have been observed on the slope 10º for loamy sand, slope

163 30^{o} for sandy loam and slope 23^{o} for silty loam because of the influence of the surface
164 roughness and micro-relief features[33–35].
165 The infiltrated volume was approximately twice in the afternoon session with temperature
166 range of 36^{o}C-42^{o}C compared to the morning session with a temperature range of 26^{o}C-32^{o}C
167 for the plain surface. Cumulative infiltration for the experiment on a 23^{o} slope surface was
168 observed 1.6 and 2.3 times higher than the plain surface under the temperature conditions of
169 morning and afternoon sessions, respectively. The cumulative infiltration was 4.6 times higher
170 for the combined effect of higher temperature and slope than the total infiltrated volume on the
171 plain surface in the morning, as depicted in Table 2.
172 Some classical infiltration models were evaluated to analyse the field infiltration
173 experiments on the Okhla landfill. Horton (HO), Kostiakov (KO), Smith (SM), Philip (PH),
174 Modified Kostiakov (MK) and SCS were selected for estimation of the model parameters using
175 observed field infiltration data. Estimated infiltration values from each focused model were
176 compared to observed data to investigate the best-suited model for inclined and plain surfaces,
177 as shown in Figure 5 and Figure 6, respectively.
178 All chosen models were fitted to the observed data from infiltration experiments using a non-
179 linear least square technique with the GRG non-linear method for infiltration rate curves.
180 Analyses of curves for the combined impacts of slope and higher temperature (Figure 5a)
181 showed that the Modified Kostiakov model was the most efficient model for infiltration rate in
182 this scenario by delivering the most optimum values of statistical parameters, as mentioned in
183 Table 4. The Horton model estimated infiltration rate reasonably good at the start and the end
184 of the process but showed a significant difference from the observed data after 10 minutes to
185 100 minutes, as shown in Figure 5(a). The Philip model exhibited the poorest results for
186 estimating initial-final infiltration rates in this scenario among all other models yet performed
187 better for cumulative infiltration estimation in the same field condition. Kostiakov model
188 obtained the most efficient performance for estimating cumulative infiltration in this scenario.

The analysis of the classical models for the combined impact of slope and higher temperature was evaluated in the performance order of KO > PH > SCS > HO > MK > SM.

Infiltration rate curves for 23º inclined surface in the morning session were generated to analyse the effects of slope, as shown in Figure 5(b). It is evident from the statistical comparison in Table 4 that Kostiakov and SCS models estimated infiltration rates closer to experimental values than other models for 23º inclined surface with a lower temperature range, as shown in Figure 5(b) as the variation of initial and final infiltration rate was observed to be 20% and 11%, respectively. The Philip model performed poorly for this situation and underestimated the initial infiltration rate by 29%. Other models have performed in the range of 'satisfactory to good' for estimating the cumulative infiltration on inclined surface in morning session in the performance order of KO > MK > SCS > HO > SM > PH.

In the morning session on the plain surface, all models overestimated the initial infiltration rates slightly, as shown in Figure 6 (a), except for Smith and SCS models. The performance of models was found to be better for plain surfaces and lower temperature range compared to the other three scenarios; although, Kostiakov and Horton outperformed in this scenario than other models and estimated the results closest to the field experimental values. In the afternoon session, all models overestimated the cumulative infiltration for the plain surface, where Kostiakov performed relatively better by showing less variation from observed values. The analysis was conducted for the estimation of infiltration rate curves in the same scenario where, Kostiakov and Horton presented better results compared to other models, as shown in Figure 6(b). As per the statistical comparison for infiltration rates in Table 4, the performance of infiltration models on plain surface in higher temperature range can be seen in the order of KO > HO > MK > PH > SM > SCS.

Initial infiltration rates were majorly dependent on soil structure, and antecedent moisture content and hence did not show a significant trend for slope and temperature variations. All the chosen infiltration models were efficient for estimating infiltration rate and cumulative

infiltration in lower temperature ranges on the plain surface (Standard situation) compared to other scenarios. The competence was least for higher temperatures and the inclined surface (combined effect of slope and temperature). Statistical analysis showed that the Kostiakov model performed relatively better than others in estimating infiltration rate and volume when temperature or slope increased.

Discussion

Temperature variation is a significant factor in the infiltration mechanism in the solid waste bulk due to exothermic reactions in the complex system[36]. The infiltration rate in the afternoon experiment session was higher than the rate observed in the morning session on plain surfaces, as depicted in Figure 4, which can be justified considering soil temperature as a function of the infiltration process[32]. As the temperature increases, more thermal movement of the water molecules is anticipated, reducing the relative mutual friction, which helps in the qualitative clarification of the reduction in viscosity and increment in hydraulic conductivity for the higher temperature[37]. Therefore, an increment in temperature raised the infiltration rate and volume for the experiments conducted in relatively higher temperature ranges[16]. Hydraulic conductivity of the local soil has proven to be the most relevant aspect of the infiltration process[38].

The solid waste in the Okhla landfill was dumped and covered by soil in a layer-on-layer structure, which created a higher possibility of subsurface flow, depending on the macro-micropores distribution in the soil matrix. The infiltration rate was higher for the inclined surface than the plain surface due to the increment in the lateral component of flow from macropores for higher inclination, which increased the gravitational potential[39]. The water infiltrated from the top layer, entering the vertical direction and flowing through the inclined permeable surface due to the gravitational force[40]. The amount of infiltrated water was significantly higher on an inclined surface in the afternoon than on the plain surface in the

morning due to the combined effects of slope and higher temperature. Previous experimental studies have observed similar results due to the rill erosion on the thin soil crust[41]. In addition, results from theoretical formulation using Green-Ampt and Richard equation have presented similar trends under ponded water conditions[42].

Model analysis displayed that all focused classical models have a problem of overestimating the infiltrated volume on the inclined surface with higher temperature ranges. The model overestimation resulted from the influence of varying depths of compacted earth cover on the solid waste. The average infiltrated volume was approximately three times higher on inclined surfaces, possibly due to thinning of the covering layer on the inclined surface. Liu noted similar overestimated outcomes through Hydraulic Bureau's equation and Chen/Lee's equation for the paddy fields[43]. Another reason for overestimation could be justified by the assumptions of homogeneous soil properties and constant moisture content throughout the surface[44].

The performance evaluation was based on estimating infiltration rates, cumulative infiltration, and overall assessment for all mentioned scenarios mentioned above. The Kostiakov and Modified Kostiakov models were the most efficient for estimating the infiltration rates and cumulative infiltration, respectively. The Kostiakov model is suited for assessing plain and inclined surfaces in lower and higher temperature ranges. Multiplying parameter of the Kostiakov infiltration model showed an increasing trend with slope and temperature increment. The same model parameter was increased at a higher rate for the experiments in the combined effects of temperature and slope. The exponent parameter of the Kostiakov model has not shown a correlation with the variations, although the values were within the range as demonstrated through previous experimental studies[12,45,46]. The multiplying parameters of the SCS model showed a similar increasing trend with the increment in opted physical features; however, the exponent showed a negative trend with the increment in slope and temperature. Zolfaghari has established similar results for the SCS model parameters on the plain surface[45].

The Horton model decay coefficient showed a negative trend with focused factors. The Philip model has not performed efficiently for the experiments in Okhla landfill except for estimating cumulative infiltration on the 23º inclined surface with the higher temperature. However, the Philip model addition parameter showed a negative correlation. Sorptivity was correlated positively with the temperature due to the reduction in surface tension and viscosity of water with temperature increment, resulting in sorptivity increment[47]. The range of sorptivity for the standard scenario was found within similar values estimated by Zolfaghari and Farid[45,46]. The limiting value of Sorptivity was analysed as 0.80 for the experimental data collected with the combined impacts of inclined surface and higher temperature. The multiplying parameter of the Modified Kostiakov model showed a similar increasing trend with slope and temperature and agreed with the experimental assessment of the Modified Kostiakov model by Zolfaghari's experiment on the plain surface[45].

Conclusion

A comparative analysis of infiltration process was evaluated for inclined surface and temperature variation on Okhla landfill based on ring-infiltrometer experimental data. The experimental data showed an increment in cumulative infiltration for the higher temperature range and higher surface inclination for ponded water. The order of classical model performance for estimating the infiltration rates in all four scenarios is MK > KO > SCS > SM > HO > PH. In the same manner, the efficiency of the models for estimating the infiltrated volume in decreasing order can be arranged as KO > SCS > MK > HO > SM > PH. Overall, the Kostiakov model showed the most efficient performance for estimating infiltration rates and infiltrated volume by generating the simulated outcomes closest to the observation data, considering the temperature and slope variation. The range of multiplying constant and exponent parameters of the Kostiakov model can be recommended from 0.10 to 0.48 and 0.38 to 0.74, respectively, for the given range of slope and temperature. The study will help select

the best suitable model and range of parameters to incorporate the effects of temperature and slope to simulate the infiltration process. Due to spatial variability, the parameters would be required to redefine the mentioned models for the heterogeneous system at a larger scale.

Disclosure Statement

Lohit Jain and Sumedha Chakma declare that they have no conflict of interest.

Data availability Statement

The raw/processed datasets generated and/or analysed during the current study of infiltration process are not publicly available as the data also forms part of an ongoing study, but are available from the corresponding author on reasonable request.

References

1. Singh, R. P., Tyagi, V. V., Allen, T., Ibrahim, M. H., and Kothari, R., An overview for exploring the possibilities of energy generation from municipal solid waste (MSW) in Indian scenario. *Elsevier*, 2011, **15**, 4797–4808.
2. Census of India 2011, *Population Projections For India And States 2011 - 2036* New Delhi, 2020.
3. *Annual Report with respect to Solid Waste Management Rules, 2016 in respect of NCT of Delhi for the Year 2016* New Delhi, 2019.
4. *Annual Report in respect of NCT of Delhi for the Year 2021-2022 on the Implementation of Solid Waste Management Rules, 2016.* New Delhi, 2022.
5. Delhi Pollution Control Council, *Compliance report of Govt. of NCT of Delhi in OA No. 606/2018* 2020.
6. Talyan, V., Dahiya, R. P., and Sreekrishnan, T. R., State of municipal solid waste management in Delhi, the capital of India. *Waste Manag.*, 2008, **28**, 1276–1287.
7. Chakma, S. and Mathur, S., Estimation of Primary and Mechanical Compression in MSW Landfills. *J. Hazardous, Toxic, Radioact. Waste*, 2012, **16**, 298–303.

8. Mukherjee, S., Mukhopadhyay, S., Hashim, M. A., and Gupta, B. Sen, Contemporary Environmental Issues of Landfill Leachate: Assessment and Remedies. *https://doi.org/10.1080/10643389.2013.876524*, 2014, **45**, 472–590.

9. Chakma, S. and Mathur, S., Postclosure Long-Term Settlement for MSW Landfills. *J. Hazardous, Toxic, Radioact. Waste*, 2013, **17**, 81–88.

10. Hopmans, J., Clausnitzer, V., and Kosugi, K. I., Evaluation of various infiltration models. *Sci. Agric.*, 1995, **140**, 5–8.

11. Haghighi, F., Gorji, M., Shorafa, M., Sarmadian, F., and Mohammadi, M. H., Evaluation of some infiltration models and hydraulic parameters. *Spanish J. Agric. Res.*, 2010, **8**, 210.

12. Sihag, P., Tiwari, N. K., and Ranjan, S., Estimation and inter-comparison of infiltration models. *Water Sci.*, 2017, **31**, 34–43.

13. Helalia, A. M., The relation between soil infiltration and effective porosity in different soils. *Agric. Water Manag.*, 1993, **24**, 39–47.

14. Mishra, S. K., Tyagi, J. V., and Singh, V. P., Comparison of infiltration models. *Hydrol. Process.*, 2003, **17**, 2629–2652.

15. Skaggs, R. W., Huggins, L., Monke, E., And Foster, G., Experimental Evaluation of Infiltration Equations. *Trans. ASAE*, 1969, **12**, 822–0828.

16. Levy, G. J., Smith, H. J. C., and Agassi, M., Water temperature effect on hydraulic conductivity and infiltration rate of soils. *South African J. Plant Soil*, 1989, **6**, 240–244.

17. Gavin, K. and Xue, J., A simple method to analyze infiltration into unsaturated soil slopes. *Comput. Geotech.*, 2008, **35**, 223–230.

18. Langhans, C., Govers, G., and Diels, J., Development and parameterization of an infiltration model accounting for water depth and rainfall intensity. *Hydrol. Process.*, 2013, **27**, 3777–3790.

19. Avudainayagam, S., Sharma, K. K., and Rajamani, V., Rate of infiltration- an in-situ measurement. *Curr. Sci.*, 1987, **13**, 663–664.

20. Fenn, D. G., Hanley, K. J., and Degeare, T. V., *Use of the water-balance method for predicting leachate generation from solid-waste-disposal sites (Technical Report) | OSTI.GOV* Washington, DC (USA), 1975.

21. Kargas, G. and Kerkides, P., A Contribution to the Study of the Phenomenon of Horizontal Infiltration. *Water Resour. Manag. 2010 254*, 2010, **25**, 1131–1141.

22. Indian Council of Agricultural Research, *Daily weather data* 2020.

23. Mohan, M. and Kandya, A., Impact of urbanization and land-use/land-cover change on diurnal temperature range: A case study of tropical urban airshed of India using remote sensing data. *Sci. Total Environ.*, 2015, **506**–**507**, 453–465.

24. SCS Engineers, Report on Assessment of Landfill Gas and Pre Feasibility Study At. 2009.

25. Gregory, J. H., Dukes, M. D., Miller, G. L., and Jones, P. H., Analysis of Double-Ring Infiltration Techniques and Development of a Simple Automatic Water Delivery System. *Appl. Turfgrass Sci.*, 2005, **2**, 1–7.

26. ASTM D3385-03, *Standard test method for infiltration rate of soils in field using double-ring infiltrometer* 2009.

27. Rocheta, V. L. S., Isidoro, J. M. G. P., and de Lima, J. L. M. P., Infiltration of Portuguese cobblestone pavements – An exploratory assessment using a double-ring infiltrometer. *http://dx.doi.org/10.1080/1573062X.2015.1111914*, 2015, **14**, 291–297.

28. Shukla, M. K., Lal, R., Owens, L. B., and Unkefer, P., Land use and management impacts on structure and infiltration characteristics of soils in the north appalachian region of ohio. *Soil sci.*, 2003, **168**, 167–177.

29. Kirkham, M. B., Chapter 13 - Infiltration. *Princ. Soil Plant Water Relations (Second Ed.*, (ed. Kirkham, M. B.), 2014, 201–227.

30. Legates, D. R. and McCabe, G. J., Evaluating the use of "goodness-of-fit" Measures in hydrologic and hydroclimatic model validation. *Water Resour. Res.*, 1999, **35**, 233–241.

31. Moriasi, D. N., Arnold, J. G., Van, L., Bingner, W., Harmel, R. D., and Veith, T. L., Model evaluation guidelines for systematic quantification of accuracy in watershed simulations. *Trans. ASABE*, 2007, **50**, 885–900.

32. Jaynes, D. B., Temperature Variations Effect on Field-Measured Infiltration. *Soil Sci. Soc. Am. J.*, 1990, **54**, 305–312.

33. Sharma, K. D., Singh, H. P., and Pareek, O. P., Rainwater infiltration into a bare loamy sand. *https://doi.org/10.1080/02626668309491980*, 2009, **28**, 417–424.

34. Mu, W., Yu, F., Li, C., et al., Effects of Rainfall Intensity and Slope Gradient on Runoff and Soil Moisture Content on Different Growing Stages of Spring Maize. *Water 2015, Vol. 7, Pages 2990-3008*, 2015, **7**, 2990–3008.

35. Khan, M. N., Gong, Y., Hu, T., et al., Effect of Slope, Rainfall Intensity and Mulch on Erosion and Infiltration under Simulated Rain on Purple Soil of South-Western Sichuan Province, China. *Water 2016, Vol. 8, Page 528*, 2016, **8**, 528.

36. Klein, R., Baumann, T., Kahapka, E., and Niessner, R., Temperature development in a modern municipal solid waste incineration (MSWI) bottom ash landfill with regard to sustainable waste management. *J. Hazard. Mater.*, 2001, **83**, 265–280.

37. Wright, P. G., The variation of viscosity with temperature. *Phys. Educ.*, 1977, **12**, 323–325.

38. Petrucci, G., De Bondt, K., and Claeys, P., Toward better practices in infiltration regulations for urban stormwater management. *Urban Water J.*, 2016, **14**, 546–550.

39. Lv, M., Hao, Z., Liu, Z., and Yu, Z., Conditions for lateral downslope unsaturated flow and effects of slope angle on soil moisture movement. *J. Hydrol.*, 2013, **486**, 321–333.

40. Miyazaki, T., *Water flow in soils* CRC Press, 2005.

41. Poesen, J., The influence of slope angle on infiltration rate and Hortonian overland flow volume. *Zeitschrift fur Geomorphol. Suppl.*, 1984, **49**, 117–131.

42. Chen, L. and Young, M. H., Green-Ampt infiltration model for sloping surfaces. *Water Resour. Res.*, 2006, **42**, 1–9.

43. Liu, C.-W., Chen, S.-K., Jou, S.-W., and Kuo, S.-F., Estimation of the infiltration rate of a paddy field in Yun-Lin, Taiwan. *Agric. Syst.*, 2001, **1**, 41–54.

44. Chahinian, N., Moussa, R., Andrieux, P., and Voltz, M., Comparison of infiltration models to simulate flood events at the field scale. *J. Hydrol.*, 2005, **306**, 191–214.

45. Zolfaghari, A. A., Mirzaee, S., and Gorji, M., Comparison of different models for estimating cumulative infiltration. *Int. J. Soil Sci.*, 2012, **7**, 108–115.

46. Farid, H. U., Mahmood-Khan, Z., Ahmad, I., et al., Estimation of infiltration models parameters and their comparison to simulate the onsite soil infiltration characteristics. *Int. J. Agric. Biol. Eng.*, 2019, **12**, 84–91.

47. Ioannou, I., Charalambous, C., and Hall, C., The temperature variation of the water sorptivity of construction materials. *Mater. Struct. Constr.*, 2017, **50**, 1–12.

411 Table 1 Classical infiltration models and parameters[12,14]

412

Infiltration model	Equations	Parameters
Kostiakov model	$f = \alpha t^{\beta}$ $F = at^{b}$	F is the cumulative infiltration, 'a' is a constant and 'b' is dimensionless positive exponent less than one. f is infiltration rate at time t. α=ab and β=b-1.
Horton model	$f_t = f_c + (f_o - f_c)e^{-kt}$	'f_t' is the infiltration time at time t, 'f_o' is initial infiltration rate (at t=0), f_c is the final constant infiltration, 'k' is a model parameter, and t is the elapsed time. 'k' is the decay constant, depends on the soil characteristics and surface cover.
Modified Kostiakov	$f_t = f_c + \alpha t^{\beta}$	f_t is the infiltration rate at time t, α and β are the constant.
SCS model	$F(t) = at^{b} + 0.6985$	a and b are the equation constants, and F is the cumulative infiltration rate.
Philip model	$f(t) = \frac{1}{2}st^{-\frac{1}{2}} + A$ $F(t) = st^{\frac{1}{2}} + At$	F(t) is cumulative infiltration till elapsed time 't'. Infiltration rate f(t), where 's' is called the sorptivity, 'A' is Philip model constant, and 't' is the elapsed time for infiltration.
Smith Model	$f(t) = f_c + A(t - t_o)^{-b}$	t_o is the time when runoff started, 'A' is the constant and 'b' is the exponent depending on the other factors governing infiltration processes such as soil characteristics, moisture content and rainfall intensity.

413

414

Table 2 Average initial and final infiltration rate for different scenario

Cases	**f_o (cm/min)**	**f_c (cm/min)**	**Slope**	**T (ºC)**
1	0.2	0.01	4º	26-32
2	0.2	0.02	4º	36-42
3	0.4	0.02	23º	30-35
4	0.4	0.05	23º	38-42

419 Table 3 Okhla landfill top layer average soil characteristics at moisture content 6.4%

420

Soil characteristics	**Measured average value (3 sets)**
Average field density on natural moisture content	1.64 gm/cc
Liquid limit	20.69%
Specific gravity	2.63
Soil type (from 0 cm to 20 cm depth)	Silty Sand (Gravel=20.37%, Sand=59.26%, Silt=14.32%, Clay=2.73%)
Maximum dry density	1.916 gm/cc at 11% moisture content
Saturated hydraulic conductivity	6.85×10^{-3} cm/min

421

422

Table 4 Statistical comparison of parameters of selected model for infiltration rate estimation on different slope and temperature ranges on Okhla landfill

Model	**parameters**		**Statistical Parameters**				**Mean temperature**	**Slope**
	α/S/k	β	R^2	RSE	PBIAS	NSE	^oC	^{o}
Kostiakov	0.100	0.439	0.917	0.178	-0.050	0.968	29^{o}C	4^o
Mod. Kostiakov	0.111	0.736	0.966	0.163	0.022	0.973		
Horton	0.693	NA	0.946	0.378	-0.299	0.857		
Smith	0.114	0.729	0.984	0.183	0.063	0.966		
SCS	0.140	0.600	0.976	0.326	0.096	0.894		
Philip	0.155	0.011	0.987	0.225	-0.010	0.949		
Kostiakov	0.225	0.390	0.934	0.290	0.010	0.913	38^{o}C	4^o
Mod. Kostiakov	0.190	0.450	0.920	0.308	0.009	0.906		
Horton	0.070	NA	0.995	0.131	-0.098	0.983		
Smith	0.200	0.465	0.913	0.326	0.106	0.894		
SCS	0.250	0.444	0.919	0.399	0.017	0.841		
Philip	0.354	0.030	0.901	0.332	0.000	0.890		
Kostiakov	0.337	0.525	0.982	0.189	0.019	0.964	33^{o}C	23^o
Mod. Kostiakov	0.320	0.650	0.966	0.250	-0.010	0.937		
Horton	0.300	NA	0.953	0.357	-0.282	0.873		
Smith	0.298	0.670	0.963	0.245	-0.088	0.940		
SCS	0.337	0.525	0.982	0.189	0.019	0.964		
Philip	0.370	0.020	0.985	0.392	-0.246	0.846		
Kostiakov	0.479	0.375	0.936	0.296	0.013	0.912	39^{o}C	23^o
Mod. Kostiakov	0.365	0.380	0.934	0.243	-0.004	0.941		
Horton	0.120	NA	0.974	0.326	-0.232	0.894		
Smith	0.370	0.420	0.923	0.266	-0.034	0.929		
SCS	0.450	0.360	0.940	0.258	-0.026	0.934		
Philip	0.800	0.065	0.900	0.332	0.008	0.890		

Note: a) temperature ranges 26 to 32 and 30 to 35 (Experiment in morning/forenoon session)
b) Temperature ranges 36 to 42 and 38 to 42 (Experiment in afternoon session)
c) S is sorptivity for philip model and k is decay coefficient for Horton model
d) α and β are multiplying and exponent parameters repectively

List of figures

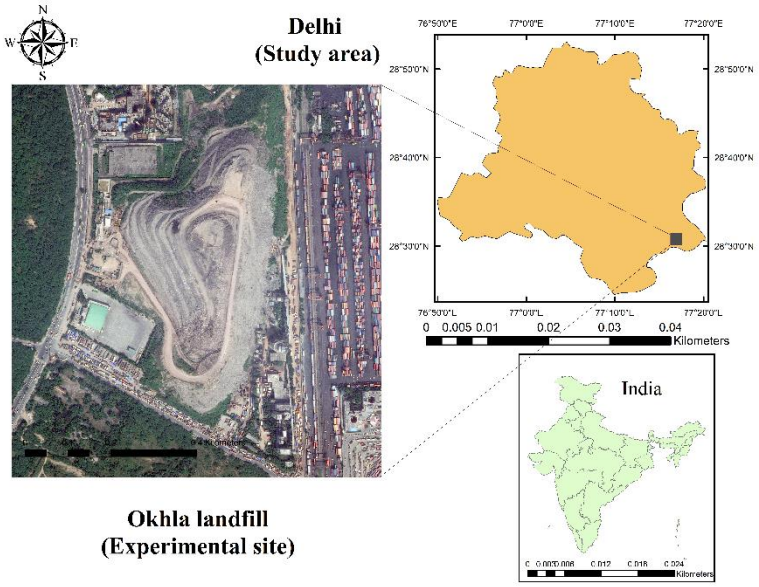

458

459 **Figure 1.** (a) Location of the study area

460

Figure 1. (b) Experimental set up at Okhla Landfill

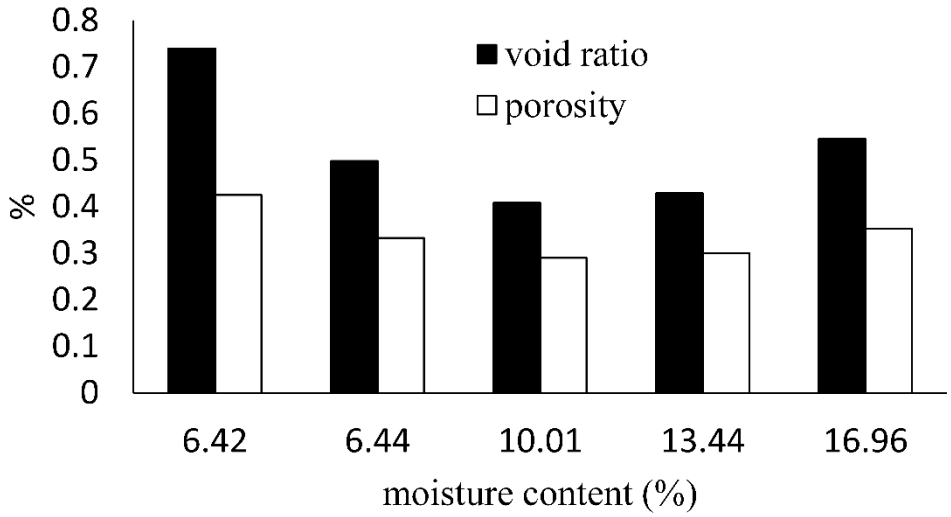

Figure 2. Porosity and void ratio variation at increasing moisture content for the Okhla top layer soil

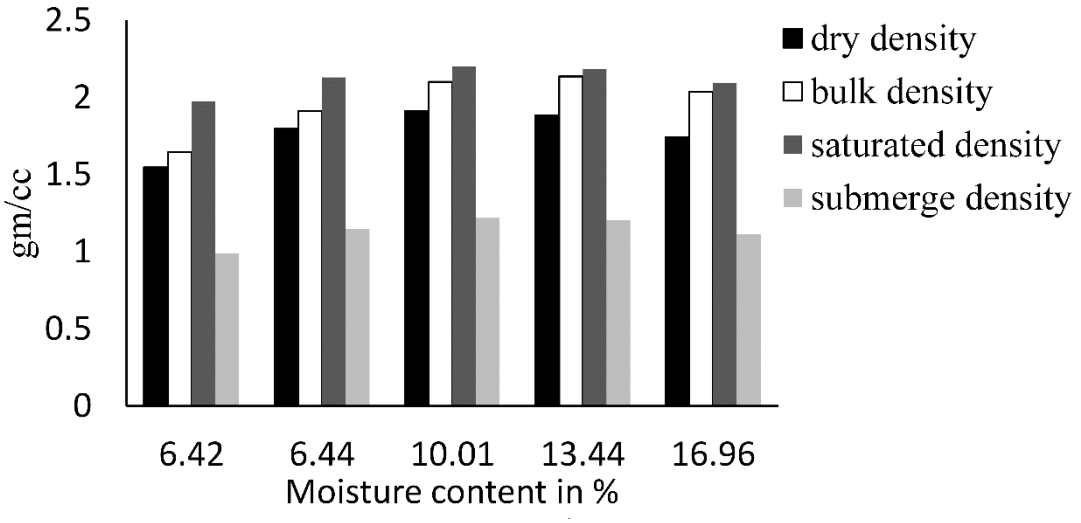

469

470 **Figure 3.** Density variations with moisture content for the top surface layer of the landfill

471

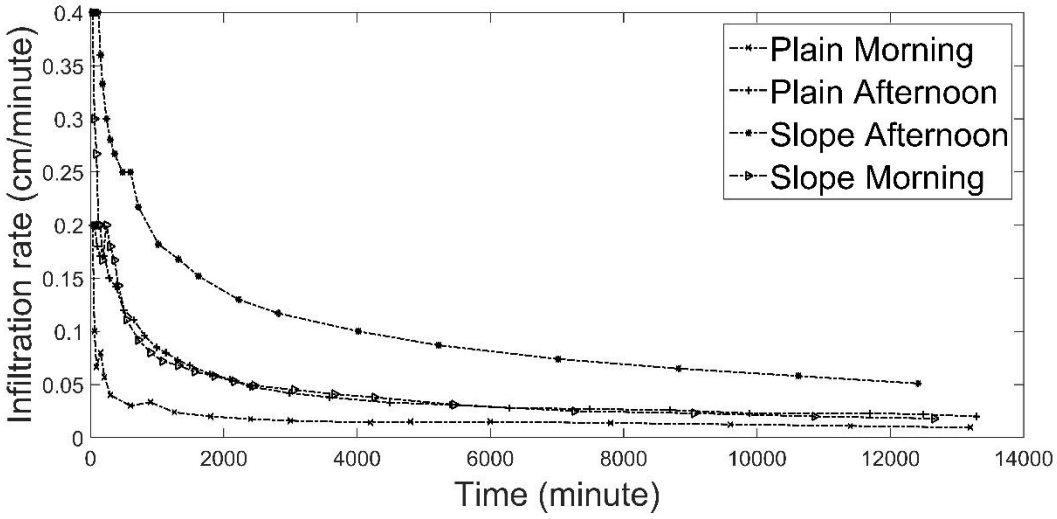

472

473 **Figure 4.** Observed infiltration rate for different slopes and temperature variation on Okhla

474 landfill

475

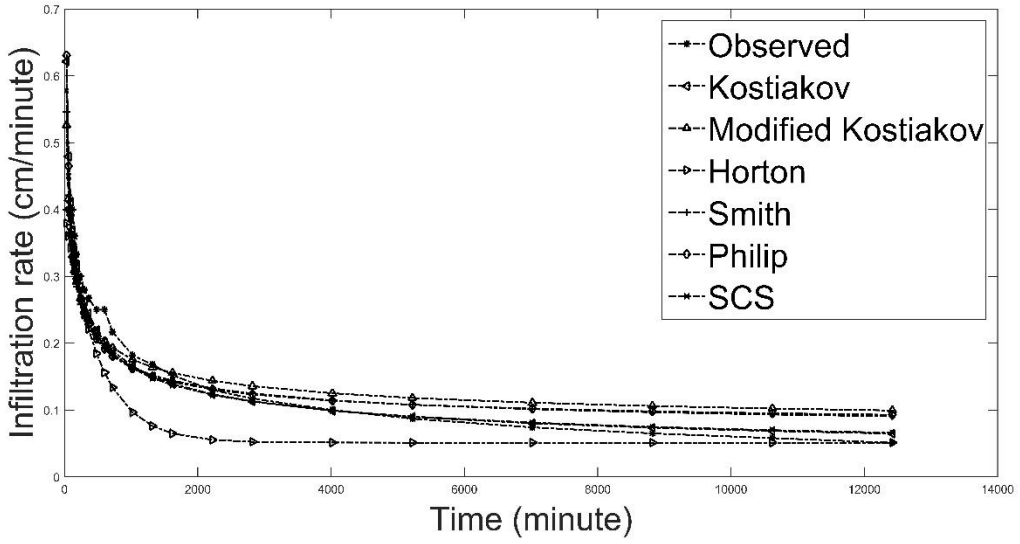

476

477

478 **Figure 5.** (a) Comparative curves of infiltration rate for slope 23º and temperature variation

479 from 38ºC to 42ºC

480

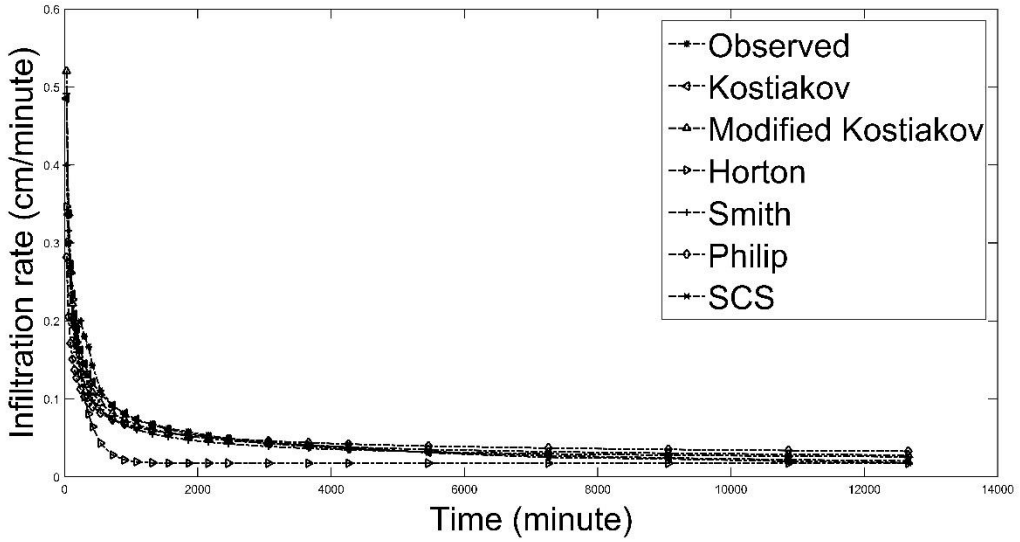

481

482

483 **Figure 5.** (b) Comparative curves of infiltration rate for slope 23^{o} and temperature variation

484 from 30^{o}Cto 35^{o}C

485

486

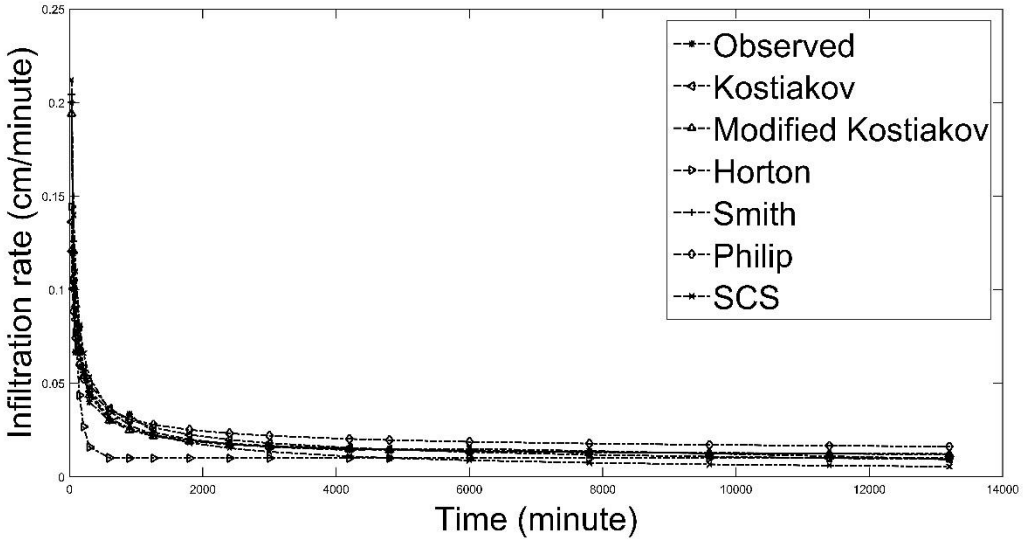

487

488

489 **Figure 6.** (a) Comparative curves of infiltration rate for slope 4^{o} and temperature variation

490 from 26^{o}C to 32^{o}C

491

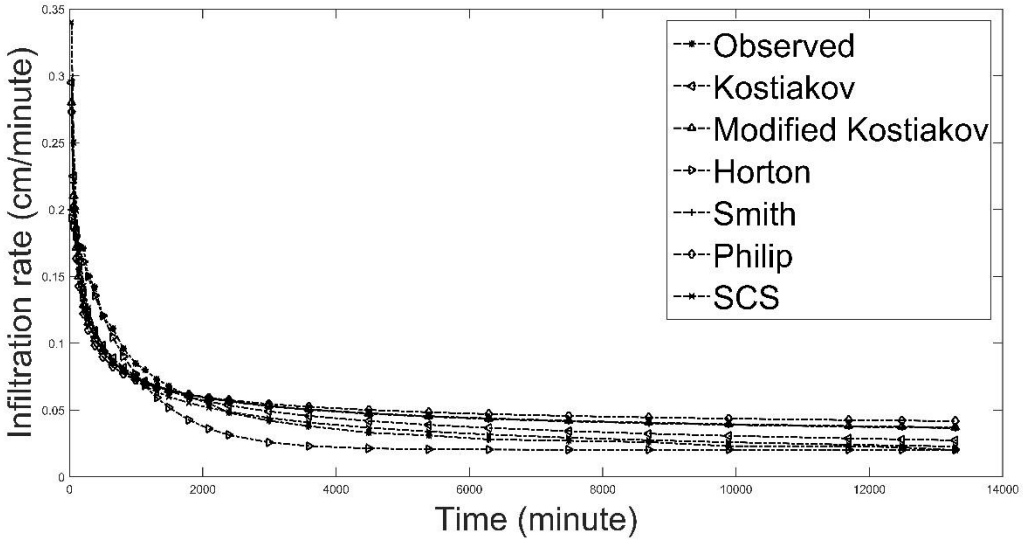

492

493

494 **Figure 6.** (b) Comparative curves of infiltration rate for slope 4^{o} and temperature variation

495 from 36^{o}C to 42^{o}C

496

497